



## On surface plasmons in porous silicon: Measurements of the electron energy loss in etched silicon nanocrystals

R. Massami Sasaki, F. Galembeck, and O. Teschke

Citation: [Applied Physics Letters](#) **69**, 206 (1996); doi: 10.1063/1.117373

View online: <http://dx.doi.org/10.1063/1.117373>

View Table of Contents: <http://scitation.aip.org/content/aip/journal/apl/69/2?ver=pdfcov>

Published by the [AIP Publishing](#)

---

### Articles you may be interested in

[Oxidefree blue photoluminescence from photochemically etched porous silicon](#)

Appl. Phys. Lett. **69**, 3779 (1996); 10.1063/1.116996

[Depth inhomogeneity of porous silicon layers](#)

J. Appl. Phys. **80**, 2990 (1996); 10.1063/1.363156

[Influence of water and alcohols on photoluminescence of porous silicon](#)

J. Appl. Phys. **79**, 7143 (1996); 10.1063/1.361484

[Pulsed anodic etching: An effective method of preparing lightemitting porous silicon](#)

Appl. Phys. Lett. **68**, 2323 (1996); 10.1063/1.115845

[Visualization of nanostructured porous silicon by a combination of transmission electron microscopy and atomic force microscopy](#)

Appl. Phys. Lett. **68**, 2129 (1996); 10.1063/1.115607

---



**AIP** | Journal of  
Applied Physics

*Journal of Applied Physics* is pleased to  
announce **André Anders** as its new Editor-in-Chief

# On surface plasmons in porous silicon: Measurements of the electron energy loss in etched silicon nanocrystals

R. Massami Sasaki and F. Galembeck  
*Instituto de Química, UNICAMP, 13081-970 Campinas SP, Brasil*

O. Teschke  
*Instituto de Física, UNICAMP, 13081-970 Campinas SP, Brasil*

(Received 7 September 1995; accepted for publication 30 April 1996)

Surface plasmons resulting from the interaction of the electron beam of a transmission electron microscope with porous silicon nanoparticles were measured. The inelastic scattering of fast electrons in H-covered silicon nanocylinders shows a peak at  $\sim 5.5$  eV. A gradual decrease of the first and second order plasma volumetric absorption simultaneous with a constant surface mode absorption amplitude was measured for decreasing silicon-slab thicknesses. Competitions between bulk and surface effects show, for the volume mode peak at 16.9 eV, a damping factor increase of  $\sim 5$  eV. The measured silicon particle diameter was  $\sim 15$  Å and a value of the dielectric constant is estimated from the surface plasmon data at 8.5, which is in agreement with recent theoretical work on the modified dielectric constant in quantum confined systems. © 1996 American Institute of Physics. [S0003-6951(96)00928-X]

Plasma losses by fast electrons in thin films have been investigated by Ritchie.<sup>1</sup> Chen *et al.*<sup>2</sup> measured the electron-energy loss spectrum (EELS) in silicon. EELS studies have been carried out on clusters of silicon spheres by Ugarte and Colliex.<sup>3</sup> Silicon spherical particles, surrounded by SiO<sub>x</sub>, show an EELS with peaks at 3, 9, 17, and 23 eV. The 9 eV contribution is due to a surface plasmon spatially sustained at the silicon-silicon oxide interface.<sup>3</sup> Batson<sup>4</sup> reported observations of inelastic scattering of fast electrons in clusters of 10–50 nm aluminum spheres that show anomalous peaks in the region 2–5 eV. A model in which the surface plasmon energy is shifted downwards from its nominal value by the strong electrostatic interaction between two adjacent small spheres was assumed.

Silicon nanostructures produced by silicon anodization in HF solutions, well described as a matrix of silicon quantum structures,<sup>5,6</sup> recently generated great interest due to the strong luminescence observed in such systems. A theoretical treatment of the dielectric constant in quantum confined systems shows that a significant value reduction takes place when the width of the quantum well is smaller than  $\sim 2$  nm.<sup>7,8</sup> In this letter we record EELS from porous silicon layers, determine the surface plasmon loss component, and estimate the value of the static dielectric constant of layers of silicon nanocrystallites.

Electron-transparent samples for transmission electron microscopy (TEM) observation were prepared by etching the silicon samples in a special electrochemical cell that produces a wedge structure.<sup>9</sup> The wedge-shaped silicon slabs were fabricated by electrochemical etching 0.5×2.0 cm pieces of silicon cut from 2-in.-diam, 0.3-mm-thick silicon wafers. The silicon piece was etched at a current density of  $\sim 200$  mA/cm<sup>2</sup> (electropolishing). The porous silicon wedge structures were also fabricated using 0.5×2.0 cm slabs. Various specimens of different thicknesses were prepared by etching slabs during different time intervals. The substrates were silicon 0.009 Ω cm, *n*-type,  $\langle 100 \rangle$ -oriented wafers. The anodization was carried out in a 25% HF solution. The con-

stant voltage was generated by a PAR 273A galvanostat/potentiostat. A drop of isopropyl alcohol was added to the tip of the silicon slab and the sample edges were gently touched by a 400 mesh TEM specimen (paralondion-coated) grid. Fragments of the silicon slab tip were transferred to the specimen grid by capillary adhesion. The grid was then dried and inserted into the TEM for study. TEM examinations were carried out in a Zeiss CEM902 microscope using 80 keV electrons and equipped with an image intensifying camera. The EELS were recorded on a TEM fitted with a Castaing-Henry filter electron spectrometer.<sup>10</sup> Energy loss spectra has an energy resolution of 1–3 eV depending on beam energy. Beam fluxes were as low as possible to minimize possible specimen damage.

Infrared absorption spectroscopy of the porous silicon layer indicates that the particles are H-terminated.<sup>11</sup> Absorption features near 1060 cm<sup>-1</sup> appear if the particles are exposed to air for a period of several minutes. In addition, no oxide-related structure in the 105–115 eV energy loss range was observed, ruling out the presence of siloxene structures.

Figure 1 shows a TEM micrograph of an *n*-type, 0.009 Ω cm,  $\langle 100 \rangle$ -oriented silicon wafer anodized for 20 min in a HF solution at a current density of 100 mA/cm<sup>2</sup>. The dark

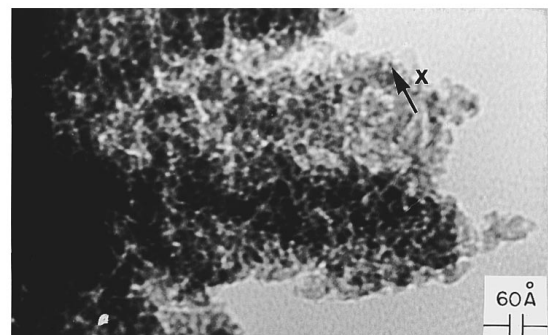


FIG. 1. Transmission electron micrograph of the porous silicon structure formed on *n*-type 0.009 Ω cm,  $\langle 100 \rangle$ -oriented silicon.  $I = 100$  mA/cm<sup>2</sup>.

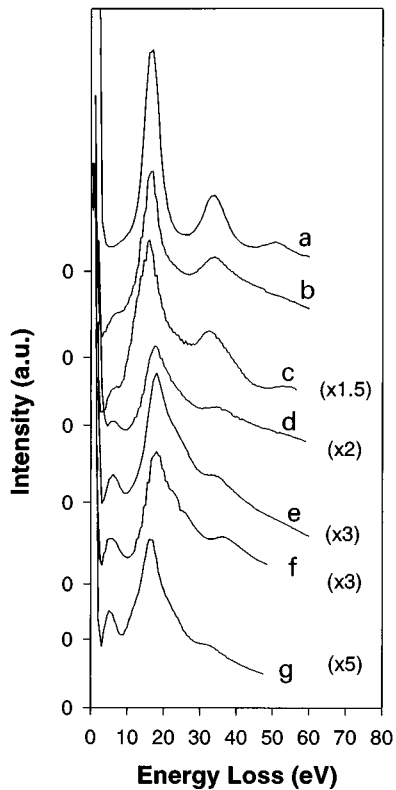


FIG. 2. EELS spectrum as a function of slab thickness. (a) silicon slab, (b) porous silicon; slab thickness  $1.29 \lambda_p$ , where  $\lambda_p$  is the plasmon mean free path,  $1.06\lambda_p$ , (c)  $0.78\lambda_p$ , (d)  $0.74\lambda_p$ , (e)  $0.60\lambda_p$ , (f)  $0.34\lambda_p$ .

areas are nontransparent to the incident electrons. A structure of pores and cylinders (or disks) that may be as small as 15 Å (indicated by X) are shown. The thicknesses of the various probed regions were calculated by measuring the ratio of the plasmon volumetric mode (integrated signal) at  $\sim 16.9$  eV ( $P_1$ ) in the zero-loss peak ( $P_0$ ) and using the following expression:  $t/\lambda_p = P_1/P_0$ , where  $t$  is the slab thickness and  $\lambda_p$  is the plasmon mean free path.<sup>12</sup>

The EELS was measured for a wedged structure of silicon. The result is shown in Fig. 2 by curve a. The observable peaks are the plasmon volumetric peaks at  $\sim 16.9$  and  $\sim 34$  eV.

Various porous silicon samples were then prepared where the contribution of the bulk plasmon absorption is gradually decreased. The measured spectra are shown in Fig. 2 by curves b–g. These curves present two distinct features: first, a peak at  $\sim 5.5$  eV shows an almost constant contribution as the sample thicknesses decrease. This is clearly shown in Fig. 3, which depicts the plasmon surface component (integrated signal) for various thicknesses of the silicon slab. Simultaneously with this effect there is a gradual decrease of the first and second plasmon bulk resonance frequency contributions. The first plasmon absorption (integrated signal) as a function of slab thickness is plotted in Fig. 3 (shown by open circles) while the surface contribution (filled circles) is shown to be independent of the slab thickness. The bulk damping factor  $\hbar\gamma = 5$  eV for a silicon slab (curve a in Fig. 2) increases to  $\sim 10$  eV for the sample formed by a skeleton of small particles (curve f). This is a

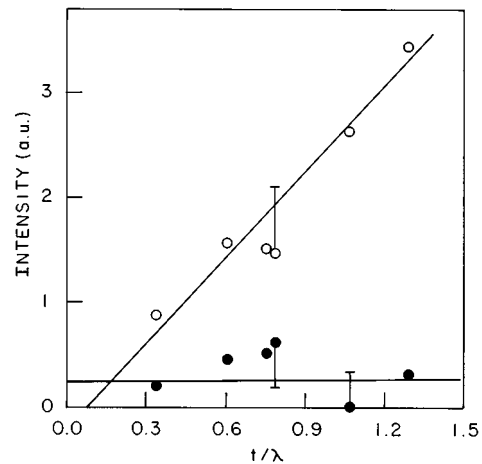


FIG. 3. Plasmon volumetric peak absorption at  $\sim 16.9$  eV (integrated signal) as a function of slab thickness (open circles). Surface plasmon absorption (filled circles).

consequence of the modes becoming a complex mixture of volume and surface losses.<sup>13</sup> Thin enough samples do not show the second plasmon absorption.

A puzzling feature about these experimental results is that the bulk losses seem to be practically the same for a silicon slab and a  $\sim \lambda_p$  thick, porous silicon slab (Fig. 2, curves a and b, respectively). The skeleton structure of 20-Å-diam particles behaves as if it is a continuous slab from a point of view of plasmon absorption. This is due probably to the interconnectivity of the grain structure forming a crystalline skeleton structure, as previously reported.<sup>14</sup> Then, since the bulk damping factor (curve a)  $\hbar\gamma = 5$  eV for a silicon slab is practically equal to the damping factor for a  $\lambda_p$  thick porous silicon slab (curve b), it is reasonable to assume that the silicon plasmon mean free path value of  $81 \pm 5$  nm is approximately equal to the plasmon mean free path for porous silicon thick slabs.

One expects losses at the lowered plasma energy to occur whenever the film or grain dimensions approach values of  $\sim v/\omega_p$ ,<sup>1</sup> where  $v$  is the electron velocity in a uniform infinite plasma and  $\omega_p$  is the plasma frequency. The low lying surface losses of Si in a cleaved monocrystal Si faces (111) has a value of 10 eV.<sup>13</sup> The value of 10 eV is in agreement with  $\hbar\omega_s = \hbar\omega_p/2^{1/2}$  ( $\hbar\omega_p = 16.9$ ). Jensen<sup>15</sup> has shown that the resonance frequency of plasma contained in a small sphere is less than the value appropriate to an infinite plasma by a factor of  $1/(3)^{1/2}$ . Figure 1 shows that porous silicon is formed by a skeleton of circular cross-sectional particles; thus, we would expect the lowered values of the losses in an actual porous silicon film to lie closer to the value  $\hbar\omega_p/(3)^{1/2}$ , appropriate to a spherical grain, than to the value  $\hbar\omega_p/(2)^{1/2}$ .

The estimated porous silicon layer dielectric constant is equal to 8.5; this value was obtained from the surface plasmon peak at 5.5 eV and<sup>13</sup>

$$\hbar\omega_s = \hbar\omega_p(1 + \epsilon)^{-1/2}, \quad (1)$$

where we consider a free electron plasma and a surrounding

porous silicon layer medium with dielectric constant  $\epsilon$ . Of course the use of the above relation is qualitative.

One may argue that the above estimate of the dielectric constant from surface plasmon measurements is reliable by using the following reasoning. Since the porous silicon layer is formed by a silicon quantum structure, its dielectric constant may be estimated by recent theoretical treatments,<sup>7</sup> as detailed below: quantum mechanical pseudopotential calculations of the static dielectric constant of silicon quantum dots predict a significant reduction relative to the bulk value for particles with  $R < 20$  Å. Particles with  $R > 30$  Å have an  $\epsilon$  value close to the  $\epsilon$  of the bulk and consequently do not have a significant effect on the surface plasmon contribution. A convenient parametrization (based on a generalization of Penn's model) of the static dielectric constant value versus particle radius  $R$  is provided by Wang and Zunger:<sup>7</sup>

$$\epsilon_s(R) = 1 + (\epsilon_b - 1) / (1 + (\alpha/R)^l), \quad (2)$$

where  $l = 1.37$  Å and  $\alpha = 6.9$  Å for the screening dielectric constant and  $\epsilon_b = 11.4$  is the silicon bulk dielectric constant. A detailed observation of silicon particles in Fig. 1 shows that diameters as small as 15 Å are observed (indicated by X). For  $R = 15$  Å measured in Fig. 1, we obtain  $\epsilon_s = 8.7$ , in close agreement with the 8.5 value previously estimated from the surface plasmon experimental data. Therefore, to account for the observed variation in the surface plasmon frequency value of porous silicon layers, we assume that the static dielectric constant corresponds to one of a quantum confined system. Consequently, the surface plasmon energy is shifted downwards from its normal value by quantum confinement of the carriers in nanoparticles.

In conclusion, the plasmon resonance absorption curves clearly show the transition from the bulk to the surface plas-

mon mode in porous silicon films as the contribution of the bulk material component is decreased. Competition between bulk and surface effects are also visible for the first and second order volume plasmons, which results in a decrease of their amplitudes and an increase in the damping factor. Quantum mechanical pseudopotential calculations show that the surface plasmon energy shift is due to quantum confinement of carriers in particles with  $R \sim 15$  Å and the estimated dielectric constant of silicon particles from the surface plasmon peak is about 8.5.

The authors would like to acknowledge helpful discussions with L. E. Oliveira. The technical assistance of J. R. Castro and L. O. Bonugli in taking some of the data is also greatly appreciated.

<sup>1</sup>R. H. Ritchie, Phys. Rev. **106**, 874 (1957).

<sup>2</sup>C. H. Chen, J. Silcox, and R. Vincent, Phys. Rev. B **12**, 64 (1975).

<sup>3</sup>U Ugarte and C. Colliex, Z. Phys. D **12**, 333 (1989).

<sup>4</sup>P. E. Baston, Phys. Rev. Lett. **49**, 936 (1982).

<sup>5</sup>L. T. Canham, Appl. Phys. Lett. **57**, 1046 (1990).

<sup>6</sup>V. Lehmann and U. Gosele, Appl. Phys. Lett. **58**, 856 (1990).

<sup>7</sup>L. Wang and A. Zunger, Phys. Rev. Lett. **73**, 1039 (1994).

<sup>8</sup>R. Tsu and D. Babić, Appl. Phys. Lett. **64**, 1087 (1994).

<sup>9</sup>O. Teschke, M. C. Gonçalves, and F. Galembeck, Appl. Phys. Lett. **63**, 1348 (1993).

<sup>10</sup>L. Reimer, I. Fromm, and R. Rennekamp, Ultramicroscopy **24**, 339 (1988).

<sup>11</sup>O. Teschke, F. Galembeck, M. C. Gonçalves, and C. U. Davanzo, Appl. Phys. Lett. **64**, 3590 (1994).

<sup>12</sup>R. F. Egerton, *Electron Energy-Loss Spectroscopy in the Electron Microscope* (Plenum, New York, 1986).

<sup>13</sup>H. Raether, in *Springer Tracts in Modern Physics*, edited by G. Höhler (Springer, Berlin, 1965), Vol. 38, p. 85.

<sup>14</sup>O. Teschke, F. Alvarez, L. R. Tessler, M. U. Kleinke, Appl. Phys. Lett. **63**, 1927 (1993).

<sup>15</sup>H. Jensen Z. Phys. **106**, 620 (1937).